Environmental Science Processes & Impacts

Sorption and Transport of Trenbolone and Altrenogest Photoproducts in Soil-Water Systems

Journal:	*Environmental Science: Processes & Impacts*
Manuscript ID	EM-ART-06-2019-000305.R1
Article Type:	Paper
Date Submitted by the Author:	28-Aug-2019
Complete List of Authors:	Yang, Xingjian; South China Agricultural University, Zhao, Haoqi (Nina); University of Washington System, Civil and Environmental Engineering Cwiertny, David; University of Iowa, Department of Civil and Environmental Engineering Kolodziej, Edward; University of Washington , Interdisciplinary Arts and Sciences; University of Washington, Civil and Environmental Engineering

Environmental significance statement. Trenbolone and altrenogest, two widely used veterinary steroidal pharmaceuticals, react rapidly (~40s - 30min half-lives) to form phototransformation products (~80% yields) upon discharge. These metastable photoproducts exhibit interesting reactivity by reforming parent structures under dark conditions (~12-24 h time scales) and also retain the potential to disrupt endocrine function. Here, we demonstrated that photoproducts exhibited reduced sorption and enhanced transport potential than parent steroids in soil-water systems, and that parent compounds can be regenerated during photoproducts transport. Therefore, the treatment efficiency of traditional agricultural runoff management practices has been overestimated when photoproducts of trienone steroids were not considered, and phototransformation can have important environmental implications on the fate of trienone steroids.

Sorption and Transport of Trenbolone and Altrenogest Photoproducts in Soil-Water Systems

Xingjian Yang[†,§,⊥,a], Haoqi Zhao[§,⊥,a], David M. Cwiertny[‖], Edward P. Kolodziej[*,‡,§,⊥]

[†]College of Natural Resources and Environment, South China Agricultural University, Guangzhou, PR China

[§]Department of Civil and Environmental Engineering, University of Washington, Seattle, Washington 98195, United States

[⊥]Center for Urban Waters, Tacoma, Washington 98421, United States

[‖]Department of Civil and Environmental Engineering, University of Iowa, Iowa City, Iowa 52242, United States

[‡]Interdisciplinary Arts and Sciences, University of Washington Tacoma, Tacoma, Washington 98421, United States

[a]The co-first authors contributed equally to this study.

*Corresponding author at: Department of Civil and Environmental Engineering, University of Washington, Seattle, Washington 98195, United States; Interdisciplinary Arts and Sciences, University of Washington Tacoma, Tacoma, Washington 98402, United States; Center for Urban Waters, Tacoma, Washington 98421, United States. Tel: (253) 692-5659

E-mail address: koloj@uw.edu (E. P. Kolodziej)

Table of contents entry

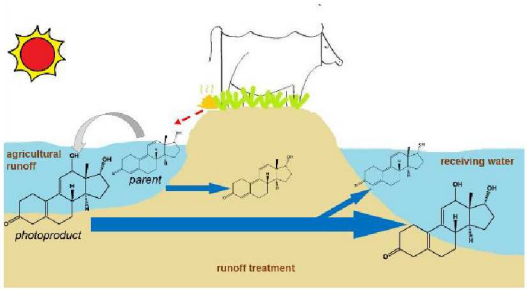

Trenbolone and altrenogest photoproducts move faster and regereate parents during transport in soil. Traditional agricultural runoff management can exhibit lower than expected efficiencies for trienone steroids when photoproducts were considered.

Abstract. This study evaluated the sorption and transport potential of seven phototransformation products of 17α-trenbolone, 17β-trenbolone, trendione, and altrenogest, along with the parent trienone steroids in batch and column soil-water systems. In batch systems, the target solutes exhibited linear isotherms, with values for sorption coefficients ($\log K_{oc}$) of parent steroids (2.46-2.76) higher than those for photoproducts (1.92-2.57). In column systems, the estimated retardation factors (R_{sol}) for parents (2.7-5.1) were ~2-5 times higher than those for photoproducts (0.84-1.7). The $\log K_{oc}$ ($R^2 = 0.75$) and R_{sol} ($R^2 =$ 0.89-0.98) were well correlated with measured $\log K_{ow}$ values, indicating that hydrophobic partitioning governed the soil-solute interaction of these biologically potent compounds in soil-water systems. These data indicated that photoproducts exhibited reduced sorption affinity and increased transport potential relative to more hydrophobic parent structures. In agroecosystems, traditional runoff management practices would be expected to exhibit reduced treatment effectiveness for photoproducts relative to the parent compounds of commonly used trienone steroids.

Keywords: phototransformation, polarity shift, solute stereochemistry, agricultural runoff treatment.

1. Introduction

The environmental discharge of potent steroidal pharmaceuticals is concerning because such compounds can disrupt endocrine function in aquatic organisms.[1, 2] Exposure to 0.8 ng/L of the progestin levonorgestrel (a human contraceptive), or 11 ng/L of the androgen 17α-trenbolone (17α-TBOH, a veterinary growth promoter), reduces fecundity in exposed fish.[3, 4] Trienone steroids, commonly used as agricultural and human pharmaceuticals[5] or performance enhancing drugs,[6] are of special concern because their conjugated trienone system greatly enhances biological potency compared to less planar steroid structures (e.g., testosterone).[7-9] Key examples include trenbolone acetate (TBA), an anabolic androgen used as growth promoter in beef cattle production,[10] and altrenogest (ALT), a synthetic progestin used as an equine and swine zootechnical pharmaceutical to maintain pregnancy, synchronize estrus for breeding, or postpone estrus after weaning.[11, 12] TBA implantation rates may exceed 20 million cattle annually in the United States,[10] with estimates of over 5000 kg production and implantation-derived revenue exceeding $1 billion.[13]

TBA is excreted into the environment as phase 1 metabolites including 17α-TBOH, 17β-trenbolone (17β-TBOH), and trendione (TBO). Of these metabolites, 17α-TBOH dominates excreted metabolite mass.[10] These metabolites are subsequently detected in agroecosystems[14, 15] and transported to surrounding environments principally via precipitation and irrigation runoff,[16] along with airborne particulate matter[17] or manure dispersal.[18] Notably, data defining the use, metabolism, and occurrence of ALT is lacking, with only a single study reporting its trace detection in municipal wastewater influent and effluent

(0.15-0.35 ng/L),[19] despite its widespread use in agricultural environments, especially for swine production.[20]

Both TBA metabolites (i.e., 17α-TBOH, 17β-TBOH and TBO) and ALT exhibit atypical phototransformations to yield a suite of potential environmental photoproducts. When exposed to sunlight, 17α-TBOH and 17β-TBOH form 5-hydroxy- and 12-hydroxy photoproducts (5- and 12-OH-17α/β-TBOH), and TBO forms a single hydroxy photoproduct (TBO-OH, hydroxyl position unconfirmed) with ~25 min half-lives and ~80% yields.[13] These photohydration products can then revert back to parent TBA metabolites in the dark via thermal dehydration,[7] forming a coupled photohydration-dehydration cycle that can reversibly convert these steroids between parent and product structures depending on environmental conditions (Figure 1a-1c). ALT experiences extremely rapid photolysis (~25 s half-life), forming a primary cycloaddition photoproduct (ALT-CAP) via photoisomerization and a secondary hydroxylated photoproduct (ALT-CAP-OH) via photohydration (half-life ~40 s).[21] Thermal dehydration also occurs for ALT-CAP-OH but only back to ALT-CAP; the initial photoisomerization is irreversible (Figure 1d).[21] Therefore, in any sunlit systems, TBA metabolites and ALT are present in agricultural runoff not only as the parent compounds but also as hydroxylated and isomeric photoproducts that can have significant contributions to the complex mixture of steroids in agro-ecosystems.

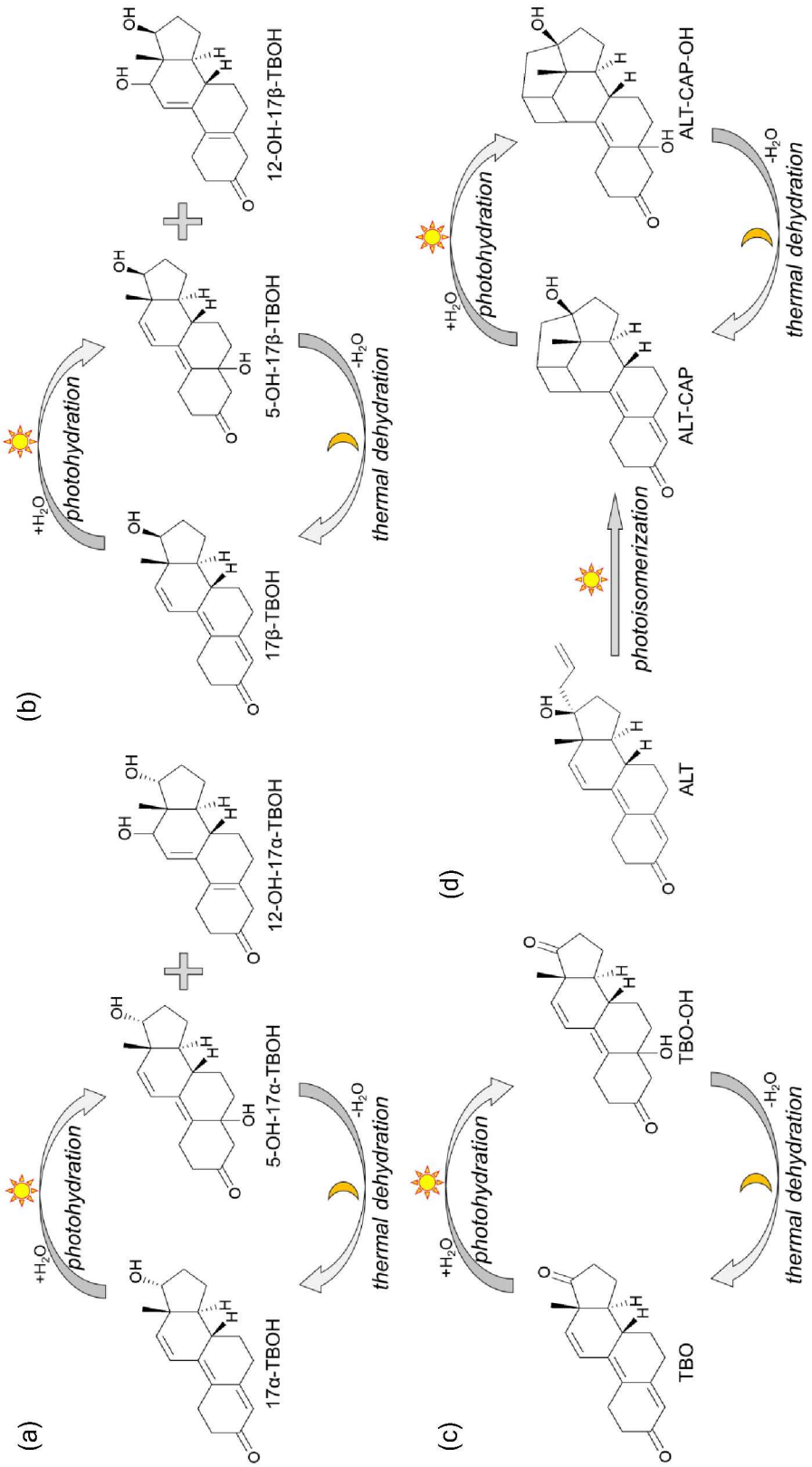

Figure 1. Structures and photoreaction dynamics of the trenbolone metabolites (a: 17α-TBOH; b: 17β-TBOH; c: TBO;) and d: altrenogest; including related photoproducts. The sun and moon symbols indicate sunlit (via a photoreactor) and dark conditions, respectively. Arrows show photoreaction pathways including photoisomerization and coupled photohydration-thermal dehydration.

Before being discharged into the environment, agricultural runoff can be subject to different management practices (e.g., vegetated infiltration basins, riparian buffers) to improve water quality. Most of these processes rely upon surface or subsurface sequestration (i.e., hydrophobic partitioning) mechanisms to limit contaminant transport.[18,22] The transport potential of contaminants in these treatment systems, which is often compared via solute breakthrough times or pore volumes in soil columns, is closely related to solute polarity.[23] For example, Goeppert et al. (2014) observed faster breakthrough of polar conjugated estrogens such as estrone-sulfate ($\log K_{ow}$ = 0.95, 4-5 pore volume) relative to less polar estrone ($\log K_{ow}$ = 3.10, 24-26 pore volume) and 17β-estradiol ($\log K_{ow}$ = 4.01, ~26 pore volume).[23] Vegetated filter strips and subsurface infiltration have been shown to be effective at attenuating TBA metabolite concentrations via partitioning to soil and organic matter.[24, 25] However, because the photohydration reactions increase compound polarity, the hydroxylated photoproducts would be expected to exhibit reduced sorption and enhanced transport potential in any of these soil-water treatment environments. Their potential for thermal dehydration also implies that highly potent parent steroids (i.e., TBA metabolites, ALT-CAP) can be regenerated during dark subsurface-treatment from more mobile photoproducts which act as metastable reservoirs of parent mass. Thus, shallow groundwater, vegetated filter strips, riparian buffers, and hyporheic zones may all exhibit reduced sequestration and treatment effectiveness for reactive trienone steroids whenever photoproducts are formed. Here in this study, we seek to better understand the possibility of such processes.

Batch and column experimental systems are often used to quantify partitioning

interactions among solutes, water, and soils during porous media transport.[26, 27] Partitioning constants and transport data have not been reported for TBA metabolite photoproducts, for ALT, or ALT photoproducts in soil-water systems. In general, few data exist that characterize sorption and transport outcomes for reactive solutes or transformation products, especially those that lack pure standards to facilitate experimentation. Therefore, our study objectives were to evaluate the sorption of TBA metabolites (17α-TBOH, 17β-TBOH and TBO), ALT, and their seven photoproducts (5/12-OH-17α/β-TBOH, TBO-OH, ALT-CAP and ALT-CAP-OH) onto a model soil and assess their short-term (several hours to 1 days, typical for runoff management systems) transport in soil columns as a model for subsurface runoff treatment. Using a novel experimental setup, we simulated coupled transformation-transport by generating photoproduct mixtures with a solar simulator and then infiltrating these mixtures to either batch soil-water systems or soil columns. These data were subsequently used to predict field scale transport potential and probable treatment efficacy for ALT, TBA metabolites, and their related photoproducts.

2. Materials and methods

2.1 Soil and water collection

A silica sand-soil mixture (95:5, *w:w*, f_{oc} = 0.06%) was used for batch and column experiments as a representative porous media (Figure 2). Loamy sand (0-30 cm) was collected in Pierce County, WA, USA (122.2827° W, 47.1295° N), with physical-chemical properties shown in Table S1. Soil was air-dried, ground, and sieved to 1 mm prior to use. Commercial grade silica sand (<1 mm diameter) was washed and used as is. The "model

water" used in all of the batch and column systems was a circumneutral (pH ≈ 7.2), low dissolved organic matter (< 2 mg/L), low ionic strength water collected from the Snoqualmie River, Ollalie State Park, WA, USA (121.6533° W, 47.4372° N). This model water was used instead of acidic LC-MS grade water (pH ≈ 5.5) to limit photoproduct reversion via acid-catalyzed dehydration (dehydration rates for 17α-TBOH: 0.17 μM $hour^{-1}$ at pH 7 vs 0.6 μM $hour^{-1}$ at pH 5),[7] to limit sodium adduct formation that can affect trienone steroid quantification, and to use environmentally relevant water compositions (e.g., natural organic matter).[28] The soil, silica sand, and model water contained no detectable steroidal analytes. Chemical and reagent sources are provided in the Supporting Information (SI).

2.2 Photoproduct quantification

Photoproduct standards are not commercially available, and we were unable to make photoproduct standards via synthetic pathways despite much effort. Therefore, calibration standards of photoproduct mixtures were generated immediately before each usage by irradiating aqueous solutions (0.05-100 μg/L) of ALT, 17α-TBOH, 17β-TBOH, and TBO that were diluted from stock solutions (in methanol, stored in amber glass vials at -20 ºC) with sterilized (autoclaving, 121 ºC, 20 min) model water (methanol content ≤ 0.01% *v/v*). The resulting solutions were mixtures of ALT-CAP and ALT-CAP-OH, 5-OH- and 12-OH-17α-TBOH, 5-OH- and 12-OH-17β-TBOH, and TBO-OH, respectively, and were used without any further separation. For quantitative treatment, photoproduct concentrations in the generated calibration standards were estimated by applying previously reported yields of the photoreactions to parent steroid concentrations.[21, 28, 29] Methodology for photoproduct

generation and liquid chromatography-tandem mass spectrometry quantification is reported in the SI and elsewhere.[28]

2.3 Solvent-Water Partitioning Coefficients

To characterize solute hydrophobicity and polarity, octanol-water (K_{ow}) and hexane-water (K_{hw}) partitioning coefficients were measured using the standard protocol from U.S. EPA (see SI).[30] As an apolar solvent, hexane interacts with solutes largely through hydrophobic interactions, while octanol, as an amphiphilic solvent, interacts with solutes through both hydrophobic and H-bonding interactions.[31]

2.4 Batch experiments

Photoproduct mixtures for batch experiments were generated from aqueous solutions of parent compounds under photoreaction conditions described above and in the SI. Sorption isotherms were conducted at five concentrations, with parent compounds of 0.1, 0.5, 1, 5, 10 μg/L and photoproducts produced from 1, 5, 10, 50, 100 μg/L parents (specific photoproduct concentrations could be estimated from reported yields of the photoreactions[21, 28, 29]). Higher parent mass was used in photoproduct generation due to low yields of some photoproducts (e.g., 6.7% yield for 5-OH-17α-TBOH) and the higher analytical method detection limits for photoproducts relative to parent compounds (Table S2). A 2 g solid (sand-soil mixture) to 8 mL water ratio was selected as an environmentally representative composition (e.g. manure lagoons)[32] and to promote solute detection in both aqueous and solid phases. Studies were conducted in duplicate at each concentration. One no-soil control and one dark control (i.e., non-irradiated parent solutions) also were included at each concentration to monitor

photoproduct stability during equilibration and to detect possible experimental artifacts (Figure 2).

Solid and aqueous phases were sterilized by autoclaving (121 ˚C, 20 min), and glassware by baking (450 ˚C, 4 h) prior to use. Batch systems were equilibrated on a rotary shaker (125 rpm) for 22 h at 4 ˚C in the dark. This temperature, lower than typical (i.e., 25 ˚C), was selected to promote photoproduct stability. Equilibration times were selected based on literature results[22] and preliminary studies designed to evaluate possible impacts of thermal dehydration on data quality (Figures S1, S2). However, the TBO-OH sorption was notably short of soil-water equilibrium at 22 h (Figure S1c), but we accepted this uncertainty because the error was within 25%. After equilibration, the systems were centrifuged (2500 rpm at 4 ˚C, 10 min), 500 µL of supernatant was withdrawn, 0.5 ng of 17β-d_3-TBOH was added as internal standard, and the solution was diluted to 1 mL with methanol. The remaining supernatant was discarded and the sand-soil mixture was spiked with 8 ng of 17β-d_3-TBOH and extracted with two 4 mL methanol aliquots under ultrasound (15 min).[10] Extracts were centrifuged and 250 µL of each supernatant was withdrawn, combined and diluted 1:1 (*v/v*) to 1 mL final volume with sterilized model water for liquid chromatography-tandem mass spectrometry analysis.[28]

The resulting sorption data were fitted to linear isotherms, including only those solutes that were detected in both aqueous and solid phases. Due to some non-detects in the soil phases (Table S4), isotherms were not estimated for 5-OH- and 12-OH-17β-TBOH.

2.5 Column experiments

Photoproducts used for soil column studies were generated by irradiating respective parents in a continuous flow photoreactor (a custom-built glass coil, 25 mm diameter, 700 mL) immersed in a water bath (8-10 °C; Figure S3). Flow rates were 2.1-2.7 mL/min (pore-water velocity = 0.11-0.16 cm/min), yielding ~5 h hydraulic retention times and >99% conversion to photoproducts (~10 half-lives) in the reactors. The selected velocity also is representative of typical runoff velocities in agroecosystems during rainfall.[33] Notably, we chose step input column experiments for this study to mimic the environmentally relevant continuous-flow scenario where parents or photoproducts occurring in runoff are infiltrated into agricultural systems with shallow subsurface flows.[25, 34, 35]

Column experiments used two stainless steel columns (15.2 cm length, 7.62 cm diameter, 690 mL volume) packed with the 95:5 (*w:w*) silica sand-soil mixture in 1-2 cm lifts, with 1.5 cm depth of coarse silica sand and 200 mesh stainless steel screens to ensure a one-dimensional flow, to prevent the clogging at the column outlet, and to prevent the splashing of the soil material.[36, 37] This silica-sand mixture composition was selected after a number of preliminary trials to enable column breakthrough over ~12 h time scales and to prevent data artifacts arising from photoproduct instability during longer column transport trials and long breakthrough trials. Six batches of column transport experiments were conducted representing various conditions, with one photoproduct column (photoreactor on, sunlit conditions) and one parent column (photoreactor off, dark conditions) for each batch (Figure 2). The 12 h time scale was representative of short term surface transport or subsurface infiltration in agricultural systems dominated by partitioning mechanisms like tile

drains or riparian buffers. Longer (~24 h) column experiments were also conducted for 17α-TBOH and ALT photoproducts to validate the results. Prior to experiments, each column was slowly wetted (4 L) for 24 h to remove air and equilibrate the system. Despite this saturation, the column systems were considered to be aerobic because of the oxygen-saturated infiltrating water and the limited biochemical oxygen demand of the experimental system.[38] Photoproducts mixtures were introduced into columns by pumping photoreactor solutions (bottom feed) into the columns; effluent samples (0.5 mL) were collected every 10-30 min and analyzed directly after dilution with methanol (1:1 v/v) and addition of 0.5 ng of 17β-d_3-TBOH. Columns were repacked with new sand-soil media between each trial.

After transport studies, each column was flushed with water (~4 L) for 24 h and hydraulically characterized using NaBr, with similar procedures as steroid transport. Briefly, 0.03 M NaBr solution was continuously pumped into each column under the same flow rates as those for transport studies, and [Br-] in the column effluent were measured with a bromide selective electrode (Hanna Co., USA).

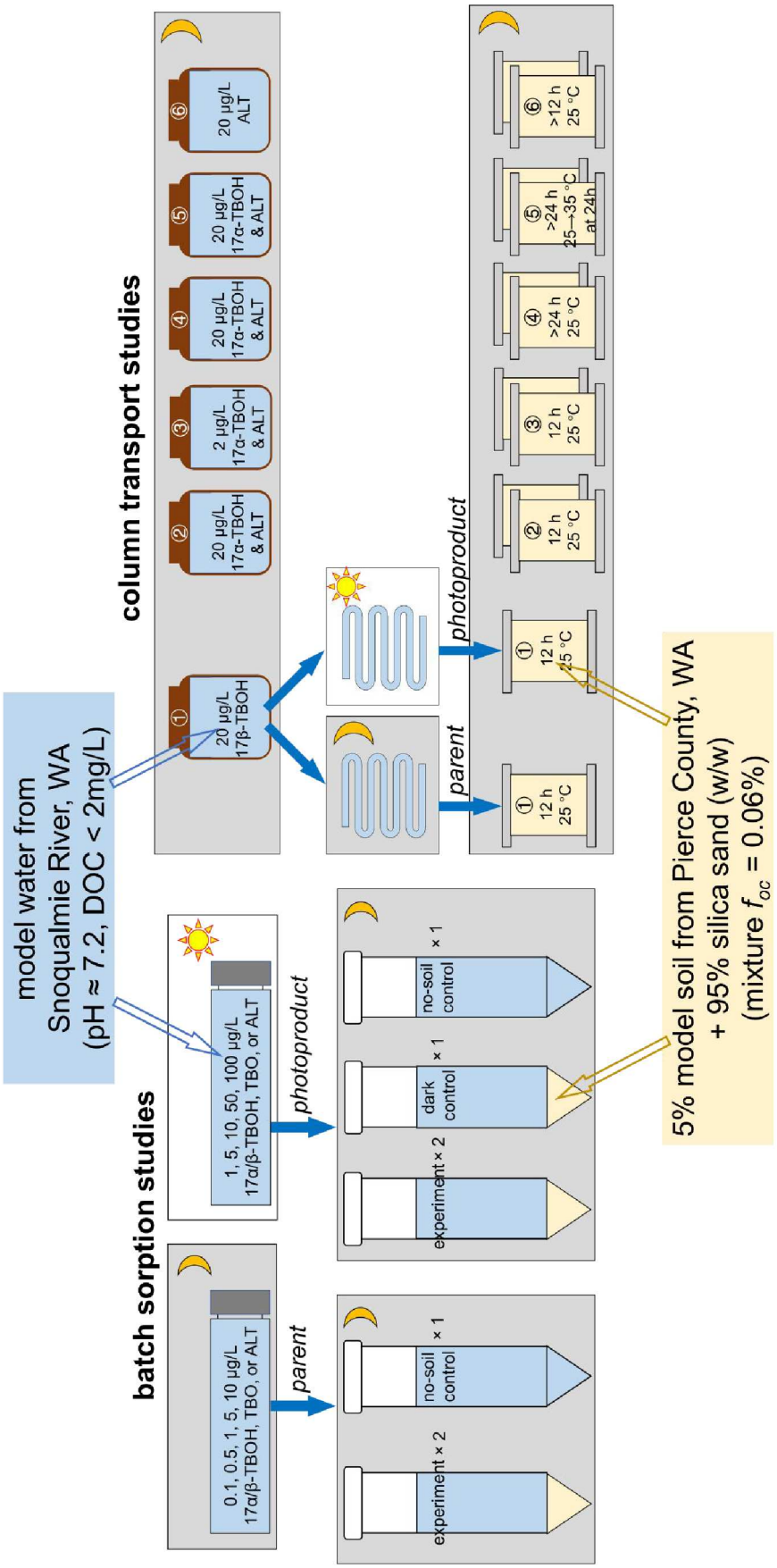

Figure 2. Overview on of the study design for both the batch sorption and column transport experiments. The sun and moon symbols indicate sunlit (via a photoreactor) and dark conditions, respectively.

2.6 Transport modelling

Column transport parameters were estimated with CXTFIT 2.1,[39] which models solute transport by equilibrium or non-equilibrium convection-dispersion equations. Detailed theories and equations of convection-dispersion equations, physical and chemical non-equilibrium models are presented in the SI. In this study, dispersion coefficient (D) and pore-water velocity (v) values were obtained by fitting breakthrough curve data of conservative tracers to the deterministic equilibrium convection-dispersion model. Then, breakthrough curve data of solutes were fitted with the chemical non-equilibrium model to estimate retardation factors (R) (i.e., R_{mod}), fraction of "Type-1" sites contributing to instantaneous sorption (β), and ratio of column hydraulic retention time to timescales for chemical partitioning (ω). Notably, β and ω can be calculated as:

$$\beta = \frac{\theta + f\rho_b K_d}{\theta + \rho_b K_d} \qquad (1)$$

$$\omega = \frac{\alpha(1-\beta)RL}{v} \qquad (2)$$

where ρ_b (g/cm^3) and θ (cm^3/cm^3) represent soil bulk density and volumetric water content, respectively. f is the fraction of exchange sites that are always at equilibrium. K_d (L/kg) is the linear distribution coefficient. α is a first-order kinetic rate coefficient (min^{-1}).

To facilitate quantitative comparison of transport potential between parents and photoproducts, R also was estimated by two other approaches.[39-41] First, a theoretical retardation factor (R_{cal}) was calculated with column parameters and sorption coefficients derived from batch systems[39]

$$R_{\text{cal}} = 1 + \frac{\rho_b K_d}{\theta} \qquad (1)$$

Alternatively, retardation factors (i.e., R_{sol}) have been estimated as the number of pore volume (or times) when the measured breakthrough curve achieved 50% recovery,[41] or by comparing the breakthrough pore volume (or time) (pore volume or time at which 50% recovery is achieved) of column solutes to that of the tracers.[40] These estimation methods were slightly modified in this study because some solutes did not attain complete breakthrough ($C/C_0 = 1$) over the 12-24 h time scales (discussed below). Here, we estimated R_{sol} as the ratio of the apparent breakthrough pore volumes of column solutes to that of the tracers: breakthrough of solutes represents the pore volumes at which solute concentrations reached half of the concentrations for the last effluent sample (i.e., last data point of breakthrough curves), and that of tracers represents the pore volumes at which tracer concentrations reached half of the equilibrium concentrations.

3. Results and discussion

3.1 Octanol-Water (K_{ow}) and hexane-water (K_{hw}) partitioning coefficients

Measured solvent-water partitioning coefficients (logK_{ow} and logK_{hw} values) for trenbolone, ALT and photoproducts were summarized in Table 1 along with published data[22, 42] and estimates by SPARC. Experimentally measured logK_{ow} and logK_{hw} values were only available for 17α-TBOH, 17β-TBOH, and TBO; the results in this study (logK_{ow}: 17α-TBOH: 2.70 ± 0.03, 17β-TBOH: 2.95 ± 0.02, TBO: 2.60 ± 0.02; logK_{hw}: 17α-TBOH: -0.29 ± 0.01, 17β-TBOH: -0.26 ± 0.02, TBO: 0.78 ± 0.04) were consistent with reported values ($\Delta\log K_{ow} <$ 0.13, $\Delta\log K_{hw} < 0.27$).[22] LogK_{ow} and logK_{hw} values of ALT were 3.74 ± 0.05 and 1.31 ± 0.02, about one log unit higher than values for TBA metabolites and consistent with ALT's larger

molar volume (via ACD/Labs Percepta Platform: ALT 269.8 cm^3; TBOH 226 cm^3, TBO 225 cm^3).

Among photoproducts, ALT photoproducts exhibited the highest logK_{ow} values (2.88-3.25), followed by 17α-TBOH (1.73-2.09), 17β-TBOH (1.64-1.83), and TBO (1.25) photoproducts. Notably, the logK_{ow} of TBO and TBO-OH showed the largest disparity (ΔlogK_{ow} of 1.35) among the observed parent-photoproduct pairs (ΔlogK_{ow}: 17α-TBOH pair, 0.61-0.97; 17β-TBOH pair, 1.12-1.31; ALT-CAP pair, 0.37). Unlike any other parent compound, TBO is only a hydrogen bond acceptor but not a donor; addition of a hydroxyl group during photoreaction allows TBO-OH to both donate and accept H-bonds and enhance hydrophilicity. Our observations also indicated that C-17 hydroxyl group stereochemistry impacts the H-bonding interactions and potentials for two-phase partitioning. Despite the inverse trend observed for parents (logK_{ow}: 17α-TBOH < 17β-TBOH), 17α-TBOH photoproducts unexpectedly exhibited higher measured logK_{ow} values than 17β-TBOH photoproducts. Unfortunately, these observations could not be extended to the hexane-water system, as logK_{hw} values for photoproducts were not available due to photoproduct non-detects in hexane even after pre-concentration.

Notably, although estimated and measured logK_{ow} values of 5-OH photoproducts were similar, estimated logK_{ow} for trenbolone, ALT, ALT-CAP, and 12-OH photoproducts were consistently higher than observed values by up to one log unit (Table 1). Thus, platforms like SPARC may struggle to accurately predict the polarity difference between parents and photoproducts or between structural isomers like 5-OH and 12-OH. In addition, while the

measured logK_{ow} and logK_{hw} values were different for 17α- and 17β- TBOH stereoisomers and the 5- and 12-OH photoproducts, SPARC could not differentiate solvent-water partitioning values for these stereoisomer pairs (Table 1). Such stereochemistry effects remain poorly resolved in most computational models (e.g. SPARC, PaDEL, KOWWIN), and relative predictions for stereoisomers should be used somewhat cautiously. Additional stereochemical resolution in such models may be merited to improve accuracy. Based on the above measured values, and consistent with our expectations of reduced partitioning and enhanced transport potential, the coupled photohydration - thermal dehydration reactions do shift hydrophobicity by logK_{ow} 0.6-1.4 in magnitude when comparing the more polar photoproducts (measured logK_{ow} of 1.25-3.25) to parents (logK_{ow} of 2.60-3.74).

Table 1. Estimated solvent-water partitioning coefficients and soil-water partitioning parameters for TBA metabolites, ALT, and related photoproducts.

	logK_{ow}			logK_{hw}			linear isotherm				
	result	*Khan et al.*[1]	SPARC	result	*Khan et al.*[1]	SPARC	mass balance (%)	R^2	K_d	logK_{oc}	*Khan et al.*[1] logK_{oc}
17α-TBOH	2.70 ± 0.03	2.72 ± 0.02	3.63	-0.29 ± 0.01	-0.114 ± 0.006	1.18	97 ± 10	0.90	1.72 ± 0.13	2.46 ± 0.03	2.77 ± 0.12
5-OH-17α-TBOH	1.73 ± 0.02	-	1.63	< -3.94[a]	-	-2.49	125 ± 9	0.99	0.50 ± 0.01	1.92 ± 0.01	NA[b]
12-OH-17α-TBOH	2.09 ± 0.06	-	3.22	< -3.55	-	0.91		0.94	0.81 ± 0.07	2.13 ± 0.04	NA
17β-TBOH	2.95 ± 0.02	3.08 ± 0.03, 3.09[2]	3.63	-0.26 ± 0.02	-0.050 ± 0.010	1.18	87 ± 11	0.91	1.88 ± 0.20	2.50 ± 0.05	3.08 ± 0.10
5-OH-17β-TBOH	1.64 ± 0.17	-	1.63	< -3.75	-	-2.49	89 ± 16	NI[c]	NI	NI	NA
12-OH-17β-TBOH	1.83 ± 0.02	-	3.22	< -5.50	-	0.91		NI	NI	NI	NA
TBO	2.60 ± 0.02	2.63 ± 0.05	3.15	0.78 ± 0.04	1.045 ± 0.033	1.9	104 ± 8	0.96	3.48 ± 0.17	2.76 ± 0.02	3.38 ± 0.19
TBO-OH	1.25 ± 0.04	-	1.58	-2.12	-	-1.72	166 ± 42	0.92	1.02 ± 0.07	2.23 ± 0.03	NA
ALT	3.74 ± 0.05	-	4.67	1.31 ± 0.02	-	2.47	102 ± 9	0.99	3.14 ± 0.07	2.72 ± 0.01	NA
ALT-CAP	3.25 ± 0.02	-	4.25	0.23 ± 0.02	-	2.13	108 ± 7	0.94	2.25 ± 0.15	2.57 ± 0.03	NA
ALT-CAP-OH	2.88 ± 0.15	-	2.5	< -3.73	-	-1.53	91 ± 29	0.99	0.71 ± 0.02	2.07 ± 0.01	NA

[1] Khan, et al. *Environ. Sci. Technol.* **2009**, *43* (23), 8827−8833.

[2] Qu, et al. *J. Agric. Food Chem.* **2014**, *62* (51), 12277-12286.

[a] Photoproducts were not detected in hexane phase. The upper limit of K_{hw} is estimated based on the instrument detection limits of photoproducts.

[b] NA = not analyzed, photoproducts were not evaluated in the previous study.

[c] NI = not included, isotherms for 17β-TBOH photoproducts were not generated due to low detection rates in soil samples.

3.2 Batch experiments

Near 100% mass recovery was observed in batch soil-water systems. Recoveries were 87 ± 11% to 104 ± 8% for parent steroids and 89 ± 16% to 166 ± 42% for photoproducts (Table 1, S3, S4). Photoproducts were not detected in dark controls and were typically stable in the no-soil controls (Table S4). However, despite silanization, recoveries for parents and photoproducts in no-soil controls were often lower (Table S3, S4) than expected. Solvent washes subsequently indicated that up to 50-65% of the input mass was sorbed onto the glassware in the absence of a competing soil matrix, and 0-30% when soil was present (Table S5). Partitioning to glassware may thus yield a slight positive bias in some partitioning estimates (overestimating partitioning potential). Such effects become evident, especially at lower input masses, via comparison to no-soil controls, and may be masked in those studies using high sorbate concentrations (μM-mM concentrations).[22, 42]

Partitioning data for TBA metabolites, ALT, and photoproducts were well approximated (R^2 >0.90) by linear isotherms (Figure 3, Table 1). Consistent with previous observations,[22, 43, 44] isotherm linearity indicated that hydrophobic partitioning dominated solute interactions with soil-sand media. Among parent TBA metabolites, TBO showed the highest sorption capacity (logK_{oc}: 2.76 ± 0.02), followed by 17β-TBOH (logK_{oc}: 2.50 ± 0.05) and 17α-TBOH (logK_{oc}: 2.46 ± 0.03), consistent with prior studies (logK_{oc}: 3.38 for TBO, 3.08 for 17β-TBOH, 2.77 for 17α-TBOH).[22] The logK_{oc} of ALT was 2.72 ± 0.01. The higher sorption potential observed for TBO is likely related to its monopolar structure (less capable of H-bond donation versus the bipolar 17α,β-TBOH), and is consistent with its higher logK_{hw}

value but weakly correlated to its lower logK_{ow} compared to 17α-TBOH and 17β-TBOH (Table 1). 17α-TBOH and 17β-TBOH showed similar capacities for sorption (ΔlogK_{oc}: 0.04), which also scaled with their similar logK_{hw} (ΔlogK_{hw}: 0.03) values but did not scale with their logK_{ow} values (ΔlogK_{ow}: 0.25). We note the sorption potentials of TBA metabolites are better estimated by logK_{hw} values rather than logK_{ow}, indicating the contribution of hydrophobic partitioning to partitioning. This observation contrasts with prior reports of logK_{oc} for 17α-TBOH and 17β-TBOH,[22] and may be a concentration dependent effect (~0.1-10 μg/L here versus ~4-500 μg/L elsewhere). 17β-TBOH exhibited higher sorption capacities than TBO in the Freundlich isotherms reported by Qu et al, (K_f: 0.98 for 17β-TBOH, 0.61 for TBO, 0.39 for 17α-TBOH), which may reflect the different soil types used or isotherm non-linearity effects (1/n of 0.63-0.85 in the Freundlich isotherms).[42]

Photoproducts, based on the K_{oc} values, sorbed by a factor of 2-3 less than parent compounds. Observed logK_{oc} values for photoproducts scaled with sorption capacities of parent steroids, with the more hydrophobic ALT photoproducts exhibiting the highest sorption capacities, followed by TBO and 17α-TBOH photoproducts (logK_{oc}: ALT-CAP (2.57 ± 0.03) > TBO-OH (2.23 ± 0.03) > 12-OH-17α-TBOH (2.13 ± 0.04) > ALT-CAP-OH (2.07 ± 0.01) > 5-OH-17α-TBOH (1.92 ± 0.01)). Notably, the observed logK_{oc} disparities were quite similar between the parent-photoproduct pairs (ΔlogK_{oc}: 17α-TBOH pair, 0.33-0.54; TBO pair, 0.53; ALT-CAP pair, 0.50) despite the larger differences in ΔlogK_{ow}. The lack of logK_{hw} values for photoproducts (discussed above) precluded further analysis.

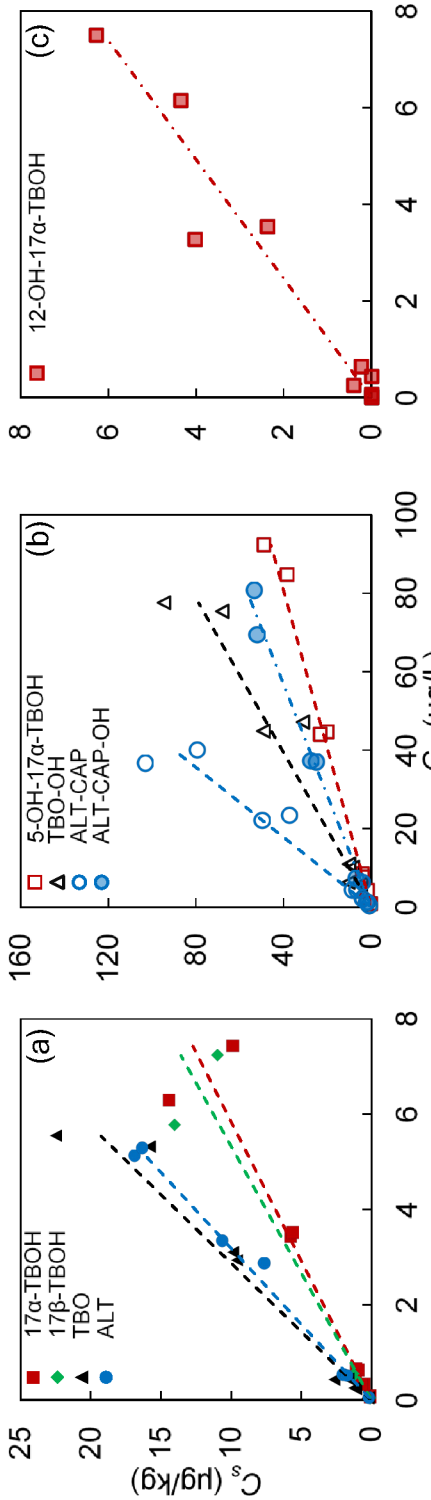

Figure 3. Linear isotherms for: (a) TBA metabolites, ALT and (b,c) related photoproducts. 12-OH-17α-TBOH had a lower concentration range in (c) due to lower photoreaction yield. C_w and C_s are aqueous and solid phase concentrations of the solutes, respectively. Note the different X and Y axis scales across the figures.

Despite the subtle difference within parent compounds, these batch studies indicate that the sorption potential of parents and photoproducts, as quantified by logK_{oc} values, generally scaled with their logK_{ow} values (p = 0.056; Figure 4a) except for TBO. Excluding TBO and TBO-OH, logK_{oc} values were significantly correlated (p <0.05) with logK_{ow} values (R^2 of 0.75, Figure 4b). This relationship was used to predict the potential mobility of moderately hydrophobic steroids under different soil-water conditions and related implications for agricultural runoff treatment. These correlations, as suggested elsewhere,[31] again imply hydrophobic partitioning as the dominant steroid-soil interaction mechanism, although the outlier behavior of TBO may arise from potential contributions of H-bonding or other specific interactions contributing to partitioning.

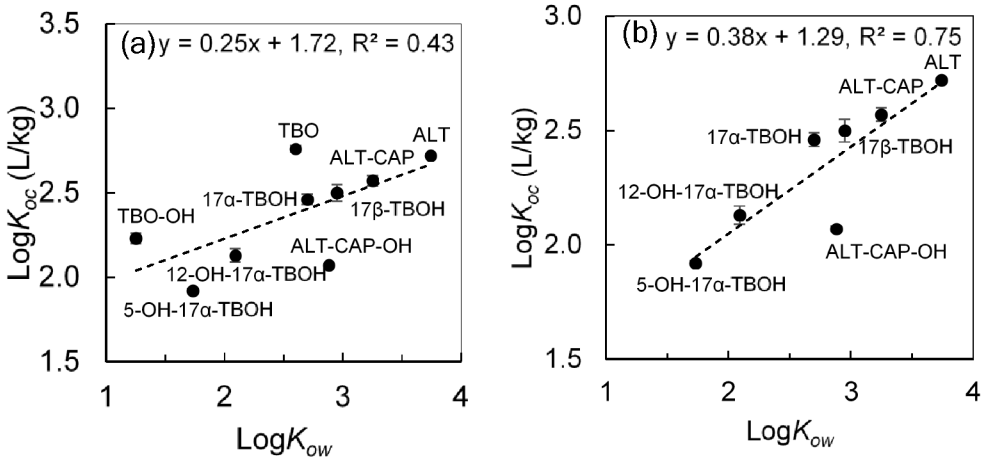

Figure 4. Observed correlations between (a) logK_{oc} and logK_{ow} of TBA metabolites, ALT, and photoproducts and (b) repeat correlations but with outlier values for TBO and TBO-OH removed. Error bars represent standard deviations.

3.3 Column experiments

Column studies were used to evaluate the transport of parents and photoproducts over ~12-24 h time scales in a coupled reaction-transport system. This dynamic scenario is expected to be environmentally relevant, in which photoproducts are generated in runoff and then be continuously infiltrated into agricultural management systems. TBO was not studied in detail due to its outlier behavior in batch systems. NaBr tracer tests (N = 8, mass recoveries of ~100%) were conducted after each column study (Table S6). Notably, the breakthrough curves of tracer were slightly shifted toward the Y-axis (Figure S4), indicating possible preferential flow in the columns.[45-47] This observation was probably due to nonuniform packing or some trapped air bubbles in the column media arising during saturation. Despite the observed preferential flow, the breakthrough curves (N =8) of tracers were well represented by the deterministic equilibrium convection-dispersion model (R^2 = 0.996-0.997, Table S6).[48] The measured (0.11-0.16 cm/min) and estimated *v* values (0.15-0.21 cm/min) for all experiments were similar, and the estimated *D* values were consistent (0.07-0.20 cm^2/min), indicating similar hydrodynamic properties during these experiments (Table S6).

Table 2. Transport parameters for target solutes in column studies derived from a two-site non-equilibrium model.

column	solute	R_{cal} [a]	R_{sol} [b]	two-site non-equilibrium model			
				R_{mod} [c]	β [e]	ω [f]	R^2
dark	17α-TBOH	7.7 ± 0.7	2.7 ± 1.2	14 ± 0.6	0.18 ± 0.02	1.4 ± 0.15	0.96-0.99
control	17β-TBOH	8.4	3.0	21	0.12	2.76	0.99
	ALT	13 ± 1.1	5.1 ± 2.2	23 ± 2	0.19 ± 0.04	2.2 ± 0.60	0.93-0.99
light	5-OH-17α-TBOH	3.0 ± 0.20	1.1 ± 0.16	NE[d]	NE	NE	0.90-0.95
	12-OH-17α-TBOH	4.2 ± 0.33	1.3 ± 0.09	NE	NE	NE	0.92-0.96
	17α-TBOH	7.8 ± 0.84	1.7 ± 0.44	NE	NE	NE	0.97-0.98
	5-OH-17β-TBOH	NE	0.84	NE	NE	NE	0.98
	12-OH-17β-TBOH	NE	1.05	NE	NE	NE	0.99
	17β-TBOH	7.7	1.26	NE	NE	NE	0.98
	ALT-CAP	9.8 ± 0.84	1.7 ± 0.47	NE	NE	NE	0.95-0.99
	ALT-CAP-OH	3.8 ± 0.26	1.0 ± 0.12	NE	NE	NE	0.84-0.99
	ALT	NE	NE	NE	NE	NE	NE

[a,c] R_{cal} and R_{mod} represent retardation factors obtained from calculation and modelling, respectively.

[b] R_{sol} represents retardation factors obtained by dividing pore volume of steroids at 50% of the concentration for the last effluent sample to that of the tracer.

[d] NE = Not estimated.

[e] β represents the fraction of "Type-1" sites contributing to instantaneous sorption

[f] ω is the ratio of column hydraulic retention time to timescales for chemical partitioning.

Column transport for parent steroids. Although breakthrough curves are usually modelled upon reaching equilibrium (i.e., complete breakthrough, $C/C_0 = 1$),[49, 50] we focused on the initial 12-24 h transport periods more characteristic of photoproduct half-lives and typical of short term field-scale scenarios (e.g., surface runoff) and agricultural management systems (12 h transport for experiment #1-3, and 24 h transport for experiment #4-6).[24, 25] Parent transport data were modeled with two-site chemical non-equilibrium models (R^2 = 0.99; Table 2, Figure 5). In "light" columns, observed parents (i.e., 17α-TBOH and 17β-TBOH) were generated only via photoproduct dehydration, resulting in higher effluent concentrations relative to influents. As the CXTFIT program cannot model such coupled photoproducts reversion-transport (or parents generation-transport) dynamics accurately, only R_{cal} and R_{sol} values were estimated for parent steroids in the light columns (discussed below). For all experiments, the observed β and ω values for parents ranged from 0.12 to 0.19 ± 0.04 and 1.4 ± 0.15 to 2.76, respectively, indicating that chemical non-equilibrium and many rate-limited "Type-2" sorption sites (≥81%) existed in the columns.[51, 52] For ~12 h column trials, the recoveries (i.e., C/C_0) of 17β-TBOH, 17α-TBOH, and ALT in dark columns were consistently ~20%, 50%, and 25% after 12 h (Figure 5a-5c). Under longer transport times (experiments #4-6, >24 h), the recoveries of 17α-TBOH and ALT in dark columns reached ~80% and 42-59%, respectively, suggesting good reproducibility across trials (Figure 5d-5f). At these timescales (<24 h), complete breakthrough was not achieved and ALT exhibited more retardation in columns relative to 17α- and 17β-TBOH. R_{mod} values for 17β-TBOH, 17α-TBOH, and ALT were 21, 14 ± 0.6, and 23 ± 2, respectively, consistent with C/C_0,

logK_{ow}, and K_{oc} trends across all parent steroids (Table 2). Notably, the ratio of observed R_{mod} for 17β-TBOH to 17α-TBOH (i.e., 1.4-1.6) in dark columns was clearly larger than the ratio of respective K_{oc} values (i.e., 1.1) derived from batch systems, indicating that solute stereochemistry clearly affects transport in porous media. As column systems had higher soil/water ratios relative to batch systems (2.4:1 versus 0.25:1), more soil mass in columns (i.e., more sites for binding) may have promoted additional interactions of 17β-TBOH to the soil (relative to 17α-TBOH), leading to more separation of 17α- and 17β-TBOH during column transport versus expectations from batch data.

R_{sol} values for 17β-TBOH, 17α-TBOH, and ALT were 3.0, 2.7 ± 1.2, and 5.1 ± 2.2, respectively, consistent with R_{mod} trends across all parent steroids and indicating that R_{sol} estimates also were accurate for these solutes and can be extended to photoproducts. For experiments #1, #2, #3, and #5, R_{sol} values for 17α-TBOH and 17β-TBOH obtained from dark control columns were larger than respective R_{sol} values for these same steroids obtained from light columns. For example, R_{sol} values for 17α-TBOH obtained from light and dark columns were 1.8 and 2.2 (experiment #2) (RSD = 14.1%), respectively, while those for 17β-TBOH obtained from light and dark columns were 1.3 and 3.0 (experiment #1), respectively. For light columns, the influent concentrations of 17α- and 17β-TBOH were very low (i.e., >99% parents transformed), so column effluent data for parent steroids were especially sensitive to dehydration (i.e., regeneration of parents during transport). R_{sol} ratio for 17β-TBOH (experiment #1) in dark control and light columns was 2.4, relative to 1.5 ± 0.3 observed for 17α-TBOH (experiment #2, 3, and 5; data not shown), which indicated that

some 17α-TBOH and 17β-TBOH regenerated from photoproducts via dehydration during transport. The data values indicate that such regenerated parents must have transported through shorter column distances relative to results from dark columns. Lower observed R_{sol} ratios for 17α-TBOH, also indicated that dehydration rates for 17α-TBOH photoproducts were faster than that for 17β-TBOH photoproducts, consistent with prior expectations.[7]

As volumetric water content and bulk density values for each column trial were similar, R_{cal} values obtained from different experiments were internally consistent (Table 2). The average R_{cal} values for 17α-TBOH, ALT, and 17β-TBOH were 7.7 ± 0.7, 13 ± 1.1, and 8.4, respectively, lower than R_{mod} obtained from modelling (14 ± 0.6, 23 ± 2, and 21, respectively) but with consistent trends as R_{mod}. As reported previously, differences in observed R_{mod} and R_{cal} values were attributed to experimental conditions and models used for batch and column systems.[53-56] For example, R_{cal} was estimated from K_d, a coefficient obtained under equilibrium conditions, whereas R_{mod} was estimated under equilibrium, physical non-equilibrium, or chemical non-equilibrium conditions that were highly dependent on the morphologies of breakthrough curves.[54] Different soil-water ratios and soil-solute contact times in batch and column systems also can contribute to disparate R_{mod} and R_{cal} values.[57] Moreover, our study modelled transport data where complete breakthrough was not achieved (i.e. we selected experimental time scales to minimize photoproduct dehydration effects), so the estimated R_{mod} values were likely to exhibit a slight high bias. Similar observations were reported elsewhere, e.g., higher R_{mod} values for sodium dodecyl benzene sulfonate and propranolol were obtained at column effluent recoveries of 60% and 50%, respectively,

relative to complete breakthrough.[49, 58] Overall, the estimated C/C_0, R_{mod}, R_{sol}, and R_{cal} data consistently indicated that ALT exhibited higher retardation (slower transport) in columns, followed by 17β-TBOH and 17α-TBOH.

Column transport for photoproducts. Interpretation of transport parameters for photoproducts was complicated by uncertainties and biases in measured photoproducts concentrations. Notably, the mass balances of photoproducts in column influents and effluents were higher than expected for the nominal masses. These observations arise from detector response variation, matrix effects arising from organic matter/ions leaching from soil columns, and the lack of pure standards or matched isotopic internal standards for the photoproducts. Also, cleanup procedures (e.g., SPE) were not employed for the column studies; samples were injected directly, which may have contributed some error.

For these cases, R_{mod}, β, and ω parameters for the photoproducts are more uncertain because CXTFIT is sensitive to solute input concentrations and the analytical challenges for metastable photoproducts preclude highly accurate quantification of input concentrations. To address this uncertainty, we only calculated R_{sol} and R_{cal} from the breakthrough curves. R_{sol} values for the photoproducts 5-OH-17α-TBOH, 12-OH-17α-TBOH, 5-OH-17β-TBOH, 12-OH-17β-TBOH, ALT-CAP-OH, and ALT-CAP were 1.1 ± 0.16, 1.3 ± 0.09, 0.84, 1.05, 1.0 ± 0.12, and 1.7 ± 0.47, respectively. Notably, R_{sol} value for 5-OH-17α-TBOH, 5-OH-17β-TBOH, 12-OH-17β-TBOH, and ALT-CAP-OH were close to or even less than 1. R_{sol} value was generally both sensitive to the breakthrough of tracer and solutes.In any column trials where complete breakthrough was not achieved, the R_{sol} values for

photoproducts were expected to be lower than those obtained under complete breakthrough conditions. Additionally, 5-OH-17α-TBOH, 5-OH-17β-TBOH, 12-OH-17β-TBOH, and ALT-CAP-OH are expected to be much more polar than their respective parents. Therefore, these combined factors have resulted in overall lower R_{sol} values of these photoproducts (i.e., R_{sol} values were near or less than 1 for these four photoproducts). In addition, the average R_{cal} for 5-OH-17α-TBOH, 12-OH-17α-TBOH, ALT-CAP-OH, and ALT-CAP were 3.0 ± 0.2, 4.2 ± 0.33, 3.8 ± 0.26, and 9.8 ± 0.84, respectively (Table 2). Consistent with their reduced hydrophobicity, all observed soil column data indicated that these photoproducts exhibited reduced retardation and faster transport in soil columns relative to parent steroids.

Within any specific column trial, logR_{sol} were moderately correlated with logK_{ow} (R^2 = 0.40-0.55, $p < 0.05$) (data not shown). In particular, correlations were especially skewed by logK_{ow} values for ALT-CAP and ALT-CAP-OH which were outliers in the dataset; stronger linear correlations between logR_{sol} and logK_{ow} values (R^2 = 0.89-0.98) were apparent if these outlier values were excluded (Figure 6). Notably, the relatively lower R_{sol} values for ALT-CAP, similar to 17α- and 17β-TBOH, was due to dehydration of ALT-CAP-OH during transport, which explains some of the outlier data. In addition, these correlations are most accurate within families of closely related structures; yet ALT-CAP and ALT-CAP-OH photoproduct structures are more distinct from the parent ALT due to the cycloaddition reaction which creates an additional steroid ring. In sum, these transport data consistently indicated that more pore volumes were needed for the more hydrophobic parent steroids to reach breakthrough and that polar photoproducts clearly have larger transport potential and

shorter breakthrough times in soil-water systems relative to their parents.

While prone to some uncertainty, we consider the R_{mod} values for parents as sufficiently accurate because they make sense and were estimated based on standard procedures.[39] In contrast, R_{sol} estimation is generally best for column systems with equilibrium transport[59] and R_{cal} is most accurate for complete sorption equilibrium in batch systems. Although these conditions were not fully met in these studies, R_{cal} and R_{sol} estimates were still included because R_{sol} and R_{cal} exhibited consistent trends as R_{mod} across all parents, indicating that these estimation approaches can be extended to photoproducts. Also, previous studies show that R_{sol} and R_{cal} values obtained under non-equilibrium conditions exhibited consistent trends as retardation factors obtained from other methods, despite potential bias caused by non-equilibrium transport or unequilibrated sorption.[59, 60] Here, we consider R_{sol} and R_{cal} methods as system-specific methods that were appropriate to compare parent and photoproduct outcomes for these column systems. We do not recommend them for direct comparison with values reported in the literature.

Consistent with diurnal cycling observed in previous studies,[7] some thermal dehydration of photoproducts occurred in the column systems during transport studies (Figure 5). For example, 17α-TBOH photoproducts exhibited 21-32% thermal dehydration (experiments #2-4) during these experiments (~12 h), whereas 17β-TBOH products yielded 4.4% dehydration (experiment #1). These data were similar to reported values for 17α-TBOH (around 20-30% reversion after 12-24 h) and 17β-TBOH (around 2% reversion after 12 h) under static conditions.[7] At longer time scales and higher temperatures (25 ˚C to 35 ˚C;

experiment #5), observed 17α-TBOH mass recovery increased from 23% (25 °C) to 58% (35 °C). These recovery data were consistent with reported dehydration rates,[7] indicating that thermal dehydration in soil-water systems was generally independent of column transport hydraulics and surface conditions. The similar dehydration rates of 17α- and 17β-TBOH photoproducts in soil columns and static water indicated no effect of sorption on dehydration, which may be due to their low partitioning affinities and their substantial dissolved fraction dominating outcomes.

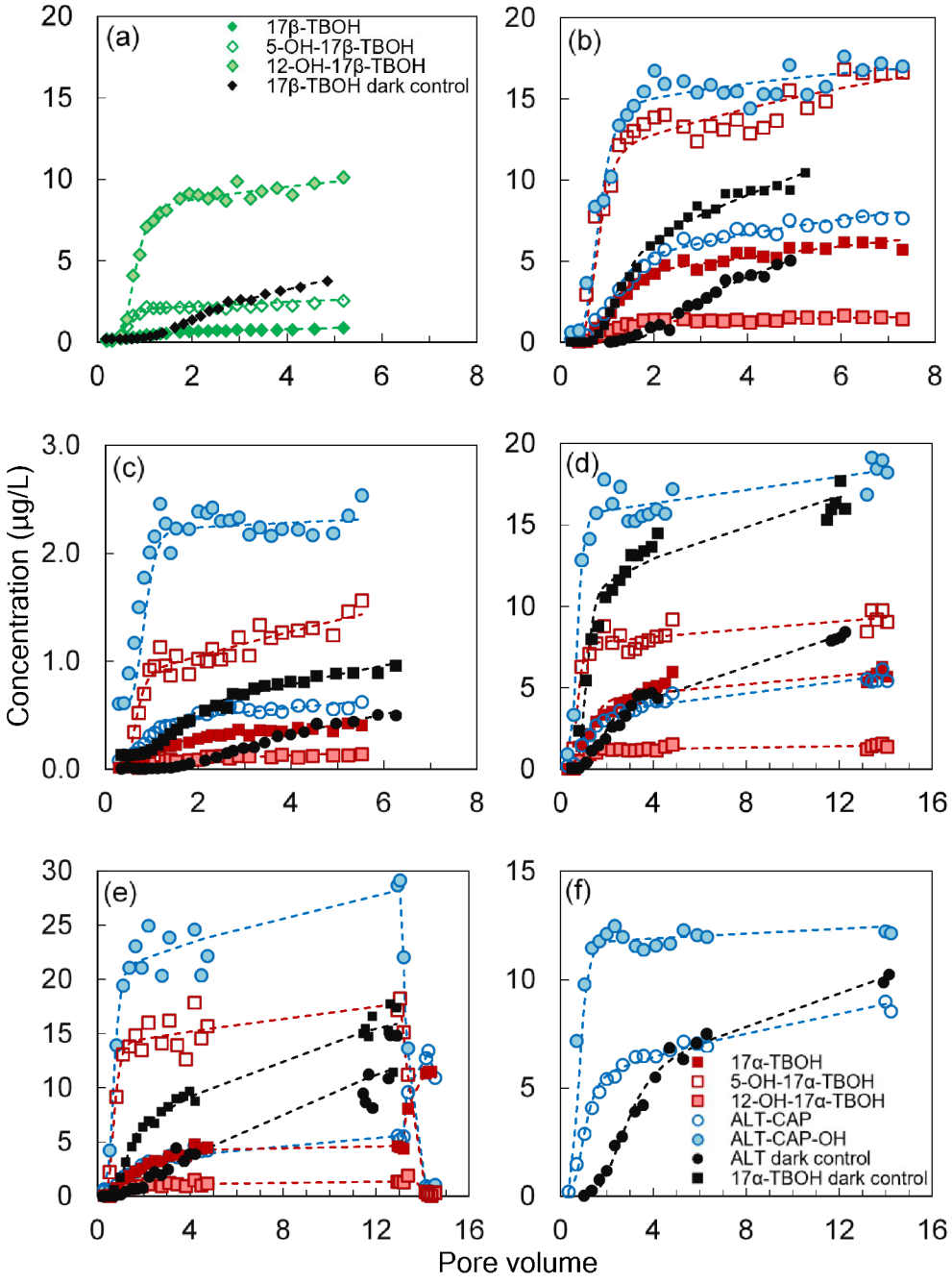

Figure 5. Observed breakthrough curves of trienone steroids and related photoproducts in soil columns. Figures 5 a-f represent experiments 1-6 (conditions described in Figure 2), respectively. To emphasize the differential transport of parent steroids versus photoproducts in the column systems, the X and Y axes were rescaled for each figure to reflect measured concentrations.

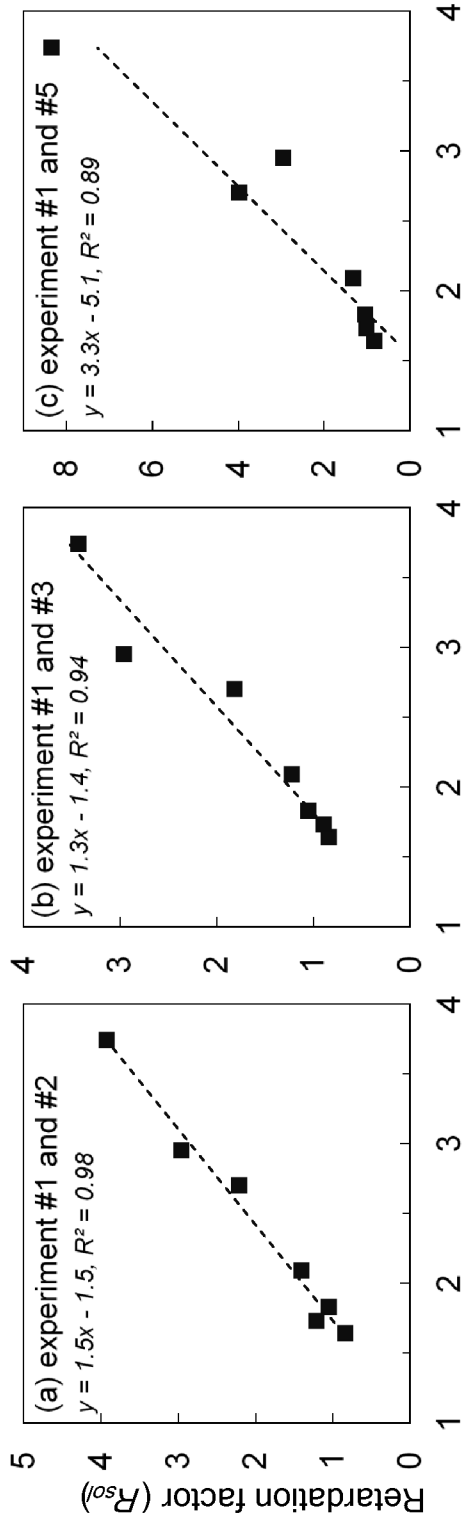

Figure 6. Observed correlations between retardation factors (as logR_{sol}) and solute hydrophobicities (as logK_{ow}). The compounds used for correlation included 5-OH-17β-TBOH, 12- OH-17β-TBOH, 5-OH-17α-TBOH, 12-OH-17α-TBOH in light columns, and 17α-TBOH, 17β-TBOH, and ALT in dark columns.

4. Environmental Implications

In this study, we evaluated batch sorption and column transport of four trienone steroids (17α-TBOH, 17β-TBOH, TBO, ALT) and their respective known photoproducts in soil-water systems. This effort investigated a dynamic reactive transport scenario where sorption, transport, and phototransformation all occur over similar time scales. We anticipate these coupled processes are important fate outcomes whenever ALT and TBA metabolites leach from animal manures and occur in sunlit surface waters (e.g., agricultural runoff, irrigation canals, vernal pools). In particular, the extreme photoreactivity of ALT, with 25-40 second half-lives to ALT-CAP and ALT-CAP-OH, respectively, suggests that photoreaction and photoproducts should dominate fate outcomes for this lightly studied potent steroid pharmaceutical, although such outcomes have not been carefully considered in directed studies.[21]

In batch systems, we observed reduced sorption of photoproducts in soil-sand mixtures relative to parents ($\log K_{oc}$ difference of parent and photoproduct: 0.33-0.65). Consistent with batch data, the estimated retardation factors from column studies were also well correlated with estimated $\log K_{ow}$ values, indicating that photoproducts exhibited reduced retardation and enhanced transport potential in soil-water systems. Therefore, building from the linear correlation between $\log K_{oc}$ and $\log K_{ow}$ ($\log K_{oc} = 0.38 \log K_{ow} + 1.29$), we estimated the expected dissolved fraction of trienone steroids ($\log K_{ow}$ = 1-4) in several soil-water systems representative of agroecosystems (Figure 7). In most surface waters (i.e., receiving river, agricultural runoff, marshes), photoproduct formation would be expected to have little effect

on the transport potential of trenione steroids due to the low availability of suspended particles for partitioning. However, for transport in agricultural systems with higher solids loadings (i.e., manure lagoon), or subsurface systems (i.e., hyporheic zones, shallow tile drain systems)[61] and treatment (i.e., infiltration basins), a unit reduction of logK_{ow} (parent median logK_{ow}: 2.83; photoproduct median logK_{ow}: 1.83) can result in 5-10% increases in water-dissolved fractions and impacts to transport. This estimate is consistent with the column transport results where photoproducts consistently exhibited 2-5 fold lower retardation factors (i.e., R_{sol}) than corresponding parents. Based on such data, we anticipate that treatment efficiencies of agricultural runoff management measures (e.g., 30-60% 17α-TBOH removal by subsurface infiltration, 70-90% by vegetative filter strips)[25] for trienone steroids would be overestimated if phototransformation was not considered. Moreover, these data indicate that parent steroids (TBA metabolites and ALT-CAP) can regenerate from photoproducts during soil-water transport, which extends the persistence of these steroids in soil-water systems.

Our previous work has demonstrated the impact of product-to-parent reversion on fate consideration of trenbolone parents, indicating that reversion cycling affects transport in systems like hyporheic zones and increases persistence and alters bioactivity of trienone steroids in surface waters.[61] Here, we demonstrate that the photohydration-dehydration cycling also increases the transport potential of trienone steroids in soil-water systems. Future studies on environmental fate of dienone and trienone steroids should consider photoproducts, including consideration of their physicochemical properties, reactivity and

transport potential, to better understand the occurrence and ecological risks of these potent pharmaceuticals.

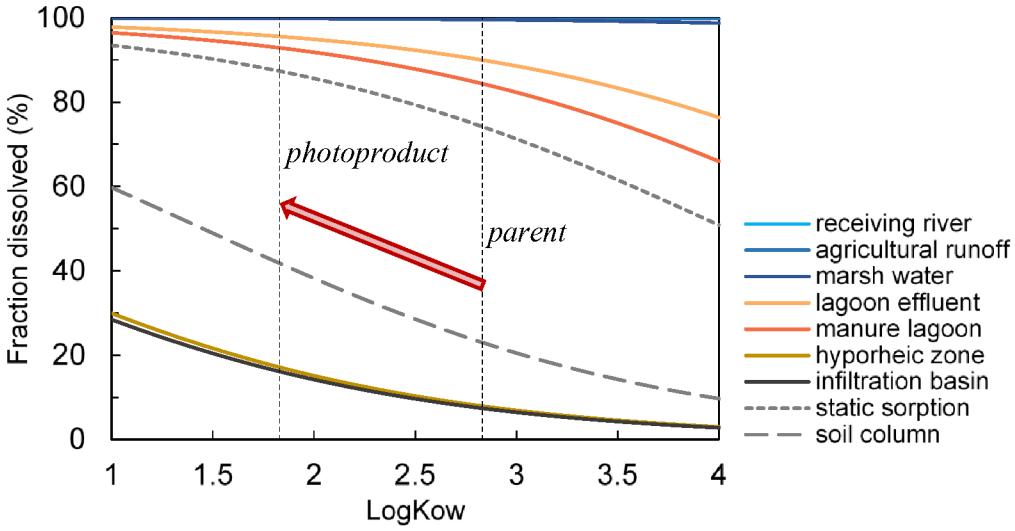

Figure 7. Predicted fraction of trienone steroids dissolved in water (i.e. mobile) as a function of logK_{ow} under conditions representative of model agro-ecosystems. Dashed black lines mark the median logK_{ow} values of the parent trienone steroids (2.83) versus values for photoproducts (1.83). The batch sorption and soil column systems represent experimental conditions described in this study. For model agricultural systems, manure lagoon and lagoon effluent represent conditions described for swine production (TSS of 2000 mg · L^{-1} for manure lagoon and 1200 mg · L^{-1} for lagoon effluent, with organic carbon content (f_{oc}) of 40%).[32, 62] Agricultural runoff, hyporheic zone, river, and marsh water represent potential transport pathways on manure-fertilized lands. The agricultural runoff and receiving water are modeled as a representative manured fields (TSS of 300 mg · L^{-1} for agricultural runoff and 100 mg · L^{-1} for receiving water, with f_{oc} of 1.3%),[63] and the hyporheic zone and marsh water conditions reflect typical reported values (hyporheic zone: porosity of 0.2, bulk density of 2.5 kg·L^{-1}, and f_{oc} of 0.5%; marsh water: TSS of 100 mg solids · L^{-1}, f_{oc} of 20%).[25] For treatment systems, subsurface infiltration conditions are modeled as those reported for a grazing rangeland (porosity: 0.47, bulk density: 1.5 kg·L^{-1}, f_{oc}: 1.7%).[31]

Funding Sources

This research was supported by United States Department of Agriculture (Grant No. 2013-67019-21365).

Conflicts of Interest

There are no conflicts of interest to declare.

References

1. G. T. Ankley, K. M. Jensen, E. A. Makynen, M. D. Kahl, J. J. Korte, M. W. Hornung, T. R. Henry, J. S. Denny, R. L. Leino and V. S. Wilson, Effects of the androgenic growth promoter 17-β-trenbolone on fecundity and reproductive endocrinology of the fathead minnow, *Environ. Toxicol. Chem.*, 2003, **22**, 1350-1360.
2. K. A. Kidd, P. J. Blanchfield, K. H. Mills, V. P. Palace, R. E. Evans, J. M. Lazorchak and R. W. Flick, Collapse of a fish population after exposure to a synthetic estrogen, *Proc. Natl. Acad. Sci.*, 2007, **104**, 8897-8901.
3. J. Zeilinger, T. Steger-Hartmann, E. Maser, S. Goller, R. Vonk and R. Länge, Effects of synthetic gestagens on fish reproduction, *Environ. Toxicol. Chem.*, 2009, **28**, 2663-2670.
4. K. M. Jensen, E. A. Makynen, M. D. Kahl and G. T. Ankley, Effects of the feedlot contaminant 17 alpha-trenholone on reproductive endocrinology of the fathead minnow, *Environ. Sci. Technol.*, 2006, **40**, 3112-3117.
5. T. Damstra, S. Barlow, A. Bergman, R. Kavlock and G. Van Der Kraak, Global assessment of the state-of-the-science of endocrine disruptors, *Geneva: World Health Organization*, 2002.
6. M. J. Geraci, M. Cole and P. Davis, New onset diabetes associated with bovine growth hormone and testosterone abuse in a young body builder, *Hum. Exp. Toxicol.*, 2011, **30**, 2007-2012.
7. S. Qu, E. P. Kolodziej, S. A. Long, J. B. Gloer, E. V. Patterson, J. Baltrusaitis, G. D. Jones, P. V. Benchetler, E. A. Cole and K. C. Kimbrough, Product-to-parent reversion of trenbolone: unrecognized risks for endocrine disruption, *Science*, 2013, **342**, 347-351.
8. W. I. P. Mainwaring, The mechanism of action of androgens, *Springer Science & Business Media*, 2012.
9. F. Neumann, Pharmacological and endocrinological studies on anabolic agents, *Environ. Qual. Saf. Suppl.*, 1975, 253-264.
10. B. Schiffer, A. Daxenberger, K. Meyer and H. Meyer, The fate of trenbolone acetate and melengestrol acetate after application as growth promoters in cattle: environmental studies, *Environ. Health Perspect.*, 2001, **109**, 1145.
11. J. Van Leeuwen, S. Williams, M. Martens, J. Jourquin, M. Driancourt, B. Kemp and N. Soede, The effect of different postweaning altrenogest treatments of primiparous sows on follicular development, pregnancy rates, and litter sizes, *J. Anim. Sci.*, 2011, **89**, 397-403.
12. C. Willmann, G. Schuler, B. Hoffmann, N. Parvizi and C. Aurich, Effects of age and altrenogest treatment on conceptus development and secretion of LH, progesterone and eCG in early-pregnant mares, *Theriogenology*, 2011, **75**, 421-428.
13. E. P. Kolodziej, S. Qu, K. L. Forsgren, S. A. Long, J. B. Gloer, G. D. Jones, D. Schlenk, J. Baltrusaitis and D. M. Cwiertny, Identification and

environmental implications of photo-transformation products of trenbolone acetate metabolites, *Environ. Sci. Technol.*, 2013, **47**, 5031-5041.

14. B. Khan and L. S. Lee, Estrogens and synthetic androgens in manure slurry from trenbolone acetate/estradiol implanted cattle and in waste-receiving lagoons used for irrigation, *Chemosphere*, 2012, **89**, 1443-1449.
15. S. Qu, E. P. Kolodziej and D. M. Cwiertny, Phototransformation rates and mechanisms for synthetic hormone growth promoters used in animal agriculture, *Environ. Sci. Technol.*, 2012, **46**, 13202-13211.
16. S. Biswas, W. L. Kranz, C. A. Shapiro, D. D. Snow, S. L. Bartelt-Hunt, M. Mamo, D. D. Tarkalson, T. C. Zhang, D. P. Shelton and S. J. van Donk, Effect of rainfall timing and tillage on the transport of steroid hormones in runoff from manure amended row crop fields, *J. Hazard. Mater.*, 2017, **324**, 436-447.
17. B. R. Blackwell, K. J. Wooten, M. D. Buser, B. J. Johnson, G. P. Cobb and P. N. Smith, Occurrence and characterization of steroid growth promoters associated with particulate matter originating from beef cattle feedyards, *Environ. Sci. Technol.*, 2015, **49**, 8796-8803.
18. B. Khan, L. S. Lee and S. A. Sassman, Degradation of synthetic androgens 17α-and 17β-trenbolone and trendione in agricultural soils, *Environ. Sci. Technol.*, 2008, **42**, 3570-3574.
19. O. Golovko, P. Šauer, G. Fedorova, H. K. Kroupová and R. Grabic, Determination of progestogens in surface and waste water using SPE extraction and LC-APCI/APPI-HRPS, *Sci. Total Environ*., 2017, **621**, 1066-1073.
20. European Medicines Agency. European public MRL assessment report (EPMAR): Altrenogest (equidaeand porcine species), EMA/CVMP/487477/2011, London, UK, 2012.
21. K. H. Wammer, K. C. Anderson, P. R. Erickson, S. Kliegman, M. E. Moffatt, S. M. Berg, J. A. Heitzman, N. C. Pflug, K. McNeill, D. Martinovic-Weigelt, R. Abagyan, D. M. Cwiertny and E. P. Kolodziej, Environmental photochemistry of altrenogest: photoisomerization to a bioactive product with increased environmental persistence via reversible photohydration, *Environ. Sci. Technol.*, 2016, **50**, 7480-7488.
22. B. Khan, X. Qiao and L. S. Lee, Stereoselective sorption by agricultural soils and liquid-liquid partitioning of trenbolone (17 alpha and 17 beta) and trendione, *Environ. Sci. Technol.*, 2009, **43**, 8827-8833.
23. N. Goeppert, I. Dror and B. Berkowitz, Detection, fate and transport of estrogen family hormones in soil, *Chemosphere*, 2014, **95**, 336-345.
24. G. D. Jones, P. V. Benchetler, K. W. Tate and E. P. Kolodziej, Trenbolone acetate metabolite transport in rangelands and irrigated pasture: Observations and conceptual approaches for agro-ecosystems, *Environ. Sci. Technol.*, 2014, **48**, 12569-12576.
25. G. D. Jones, P. V. Benchetter, K. W. Tate and E. P. Kolodziej, Surface and

subsurface attenuation of trenbolone acetate metabolites and manure-derived constituents in irrigation runoff on agro-ecosystems, *Environ. Sci.: Processes Impacts*, 2014, **16**, 2507-2516.

26. F. X. Casey, J. Simunek, J. Lee, G. L. Larsen and H. Hakk, Sorption, mobility, and transformation of estrogenic hormones in natural soil, *J. Environ. Qual.*, 2005, **34**, 1372-1379.

27. N. Goeppert, I. Dror and B. Berkowitz, Spatial and temporal distribution of free and conjugated estrogens during soil column transport, *Clean-Soil Air Water*, 2017, **45**, 11.

28. P. T. Kenyon, H. Zhao, X. Yang, C. Wu, D. M. Cwiertny and E. P. Kolodziej, Detection and quantification of metastable photoproducts of trenbolone and altrenogest using liquid chromatography-tandem mass spectrometry, *J. Chromatogr. A*, 2019, **1603**, 150-159.

29. J. Baltrusaitis, E. V. Patterson, M. O'Connor, S. Qu, E. P. Kolodziej and D. M. Cwiertny, Reversible photohydration of trenbolone acetate metabolites: mechanistic understanding of product-to-parent reversion through complementary experimental and theoretical approaches, *Environ. Sci. Technol.*, 2016, **50**, 6753-6761.

30. S. W. Karickhoff, Brown, D. S, Determination of octanol/water distribution coefficients, water solubilities, and sediment/water partition coefficients for hydrophobic organic pollutants, *EPA-600/4-79-032, Environmental Research Laboratory, Office of Research and Development, U.S. Environmental Protection Agency: Washington, DC*, 1979.

31. R. P. Schwarzenbach, P. M. Gschwend and D. Imboden, *Environmental organic chemistry*, 2019.

32. S.-S. Liu, G.-G. Ying, Y.-S. Liu, Y.-Y. Yang, L.-Y. He, J. Chen, W.-R. Liu and J.-L. Zhao, Occurrence and removal of progestagens in two representative swine farms: Effectiveness of lagoon and digester treatment, *Water Res.*, 2015, **77**, 146-154.

33. H. Blanco-Canqui, C. Gantzer, S. Anderson, E. Alberts and A. Thompson, Grass barrier and vegetative filter strip effectiveness in reducing runoff, sediment, nitrogen, and phosphorus loss, *Soil Sci. Soc. Am. J.*, 2004, **68**, 1670-1678.

34. J. P. Webster, S. C. Kover, R. J. Bryson, T. Harter, D. S. Mansell, D. L. Sedlak and E. P. Kolodziej, Occurrence of trenbolone acetate metabolites in simulated confined animal feeding operation (CAFO) runoff, *Environ. Sci. Technol.*, 2012, **46**, 3803-3810.

35. X. Zhao and W.-S. J. C. Lung, Modeling the fate and transport of 17β-estradiol in the South River watershed in Virginia, *Chemosphere*, 2017, **186**, 780-789.

36. N. Tuxen, ., P. L. Tüchsen, K. Rügge, ., H. J. Albrechtsen and P. L. Bjerg, Fate of seven pesticides in an aerobic aquifer studied in column experiments,

Chemosphere, 2000, **41**, 1485-1494.

37. M. Unold, R. Kasteel, J. Groeneweg and H. Vereecken, Transport and transformation of sulfadiazine in soil columns packed with a silty loam and a loamy sand, *J. Contam. Hydrol.*, 2009, **103**, 38-47.

38. https://www.usgs.gov/special-topic/water-science-school/science/dissolved-oxygen-and-water?qt-science_center_objects=0#qt-science_center_objects.

39. N. Toride, The CXTFIT code for estimating transport parameters from laboratory or field tracer experiments. Version 2.0, *U.S. Salinity Laboratory Res. Rep.*, 1995.

40. Y. Chen, M. A. Glaus, L. L. Van and U. Mäder, Transport of low molecular weight organic compounds in compacted illite and kaolinite, *Chemosphere*, 2018, **198**, 226.

41. R. Lal and M. Shukla, *Principle of Soil Physics*, 2004.

42. S. Qu, E. P. Kolodziej and D. M. Cwiertny, Sorption and mineral-promoted transformation of synthetic hormone growth promoters in soil systems, *J. Agric. Food. Chem.*, 2014, **62**, 12277-12286.

43. L. S. Lee, T. J. Strock, A. K. Sarmah and P. S. Rao, Sorption and dissipation of testosterone, estrogens, and their primary transformation products in soils and sediment, *Environ. Sci. Technol.*, 2003, **37**, 4098-4105.

44. G. G. Ying and R. S. Kookana, Sorption and degradation of estrogen-like-endocrine disrupting chemicals in soil, *Environ. Toxicol. Chem.*, 2005, **24**, 2640.

45. B. W. Murphy, T. B. Koen, B. A. Jones, L. M. Huxedurp, B. W. Murphy, T. B. Koen, B. A. Jones and L. M. Huxedurp, Temporal variation of hydraulic properties for some soils with fragile structure, *Soil Res.*, 1993, **31**, 179-197.

46. G. Yousefi, A. Safadoust, A. A. Mahboubi, B. Gharabaghi, M. R. Mosaddeghi, B. Ahrens and H. Shirani, Bromide and lithium transport in soils under long-term cultivation of alfalfa and wheat, *Agr. Ecosyst. Environ.*, 2014, **188**, 221-228.

47. B. Gharabaghi, A. Safadoust, A. A. Mahboubi, M. R. Mosaddeghi, A. Unc, B. Ahrens and G. Sayyad, Temperature effect on the transport of bromide and E. coli NAR in saturated soils, *J. Hydrol.*, 2015, **522**, 418-427.

48. P. Zhao, X. Zhang, C. Sun, J. Wu and Y. Wu, Experimental study of conservative solute transport in heterogeneous aquifers, *Environ. Earth Sci.*, 2017, **76**, 421.

49. B. Song, P. Xu, G. Zeng, J. Gong, X. Wang, J. Yan, S. Wang, P. Zhang, W. Cao and S. Ye, Modeling the transport of sodium dodecyl benzene sulfonate in riverine sediment in the presence of multi-walled carbon nanotubes, *Water Res.*, 2017, **129**, 20.

50. O. Lorphensri, D. A. Sabatini, T. C. G. Kibbey, K. Osathaphan and C. Saiwan, Sorption and transport of acetaminophen, 17 α -ethynyl estradiol, nalidixic

acid with low organic content aquifer sand, *Water Res.*, 2007, **41**, 2180-2188.

51. S. Baskaran, N. S. Bolan, A. Rahman and R. W. Tillman, Non-equilibrium sorption during the movement of pesticides in soils, *Pestic. Sci.*, 1996, **46**, 333-343.

52. M. L. Brusseau, R. E. Jessup and P. S. C. Rao, Modeling the transport of solutes influenced by multiprocess nonequilibrium, *Harper & Row*, 1989.

53. J. M. Marínbenito, M. J. Sánchezmartín, J. M. Ordax, K. Draoui, H. Azejjel and M. S. Rodríguezcruz, Organic sorbents as barriers to decrease the mobility of herbicides in soils. Modelling of the leaching process, *Geofis. Int.*, 2018, **313**, 205-216.

54. J. M. Marín-Benito, C. D. Brown, E. Herrero-Hernández, M. Arienzo, M. J. Sánchez-Martín and M. S. Rodríguez-Cruz, Use of raw or incubated organic wastes as amendments in reducing pesticide leaching through soil columns, *Sci. Total Environ.*, 2013, **463-464**, 589.

55. M. Larsbo, E. Löfstrand, D. V. De and B. Ulén, Pesticide leaching from two Swedish topsoils of contrasting texture amended with biochar, *J. Contam. Hydrol.*, 2013, **147**, 73-81.

56. T. C. D. Bosco, S. C. Sampaio, S. R. M. Coelho, M. M. Corrêa, A. M. Netto and N. J. Cosmann, The influence of organic matter from swine wastewater on the interaction and transport of alachlor in soil, *Acta Sci. Agron.*, 2013, **35**, 277-286.

57. H. Vereecken, J. Vanderborght, R. Kasteel, M. Spiteller, A. Schäffer and M. Close, Do lab-derived distribution coefficient values of pesticides match distribution coefficient values determined from column and field-scale experiments? A critical analysis of relevant literature, *J. Environ. Qual.*, 2011, **40**, 879-898.

58. C. Bertelkamp, J. Reungoat, E. R. Cornelissen, N. Singhal, J. Reynisson, A. J. Cabo, J. P. V. D. Hoek and A. R. D. Verliefde, Sorption and biodegradation of organic micropollutants during river bank filtration: A laboratory column study, *Water Res.*, 2014, **52**, 231-241.

59. P. Nkedi-Kizza, P. S. C. Rao, A. G. J. E. s. Hornsby and technology, Influence of organic cosolvents on leaching of hydrophobic organic chemicals through soils, *Environ. Sci. Technol.*, 1987, **21**, 1107-1111.

60. D. C. Bouchard, A. L. Wood, M. L. Campbell, P. Nkedikizza and P. S. C. Rao, Sorption nonequilibrium during solute transport, *J. Contam. Hydrol.*, 1988, **2**, 209-223.

61. A. S. Ward, D. M. Cwiertny, E. P. Kolodziej and C. C. Brehm, Coupled reversion and stream-hyporheic exchange processes increase environmental persistence of trenbolone metabolites, *Nat. Commun.*, 2015, **6**, 7067.

62. G. F. Huang, Q. T. Wu, J. W. C. Wong and B. B. Nagar, Transformation of organic matter during co-composting of pig manure with sawdust, *Bioresour. Technol.*, 2006, **97**, 1834-1842.

816 63. T. E. Jordan, D. F. Whigham, K. H. Hofmockel and M. A. Pittek, Nutrient and
817 sediment removal by a restored wetland receiving agricultural runoff, *J.*
818 *Environ. Qual.*, 2003, **32**, 1534-1547.